Penerbit Akademia Baru

Journal of Advanced Research in Applied Sciences and Engineering Technology

www.akademiabaru.com/ submit/index.php/araset/index
ISSN: 2462-1943

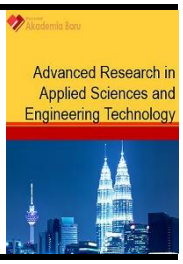

Pulsatile CFD Numerical Simulation to investigate the effect of various degree and position of stenosis on carotid artery hemodynamics

Thineshwaran Subramaniam[1], Mohammad Rasidi Rasani[1,*]

[1] Department of Mechanical and Manufacturing Engineering, Faculty of Engineering and Built Environment, Universiti Kebangsaan Malaysia, 43600 UKM Bangi, Selangor, Malaysia

ABSTRACT

This study is intended to investigate the effect of various degree and position (pre-bifurcation and post-bifurcation) of stenosis on carotid artery hemodynamics trough realistic CFD numerical simulations with appropriate turbulence model. The blood rheological properties were assumed as incompressible and Newtonian fluid. A 3 dimensional model of a non-stenotic carotid artery model was used this investigation. Several turbulence model were tested. The non-stenotic artery geometry was altered as 30% and 70% pre-bifurcation stenosis model, 30% and 70% post-bifurcation stenosis model. Pulsatile simulations were conducted for the non-stenotic and each stenotic artery models. The SST k-ω with Low-Reynolds number was found to be more appropriate for the simulation. As the degree of pre-bifurcation stenosis increases from 30% to 70%, the ICA maximum velocity increases from 12% to 65%. Also, the ECA maximum velocity increases from 5% to 45%. Besides, the ICA velocity ratio decreases by 22% but the ECA velocity ratio increases by 101%. As the degree of post-bifurcation stenosis increases, the ICA maximum velocity takes a longer time to decrease after the peak systole velocity and the ECA maximum velocity becomes higher than a non-stenotic artery throughout the cardiac cycle. A mild stenosis at post-bifurcation does not show much effect on the carotid artery hemodynamics. However, even a mild stenosis at pre-bifurcation resulted in fluctuating maximum velocity at both ICA and ECA, especially during the diastole of the cardiac cycle.

Keywords:
Carotid artery stenosis; Hemodynamics;
Computational fluid dynamics

Received: 13 March 2021 **Revised: 15 April 2022** **Accepted: 18 April 2022** **Published: 19 April 2022**

1. Introduction

Atherosclerosis has been one of the leading causes of death worldwide, accounting for millions of deaths every year. Particularly, the narrowing or obstruction of arteries due to build up plaque is the major cause of the diseases. Carotid artery bifurcation which forks the blood flow into two, Internal Carotid Artery (ICA) and External Carotid Artery (ECA) are seriously

* *Corresponding author.*
E-mail address: rasidi@ukm.edu.my

https://doi.org/10.37934/araset.26.2.2940

affected by atherosclerosis due to its geometry that allows plaque to deposit easily compared to a straight blood flow [1]. Computational Fluid Dynamics (CFD) numerical simulation is a valid approach to solve and analyze problems that involve blood flow, since it can replicate results in agreement with those obtained in in-vivo studies [24]. Carrying out such simulations require accurate anatomic models, imposition of realistic boundary conditions, utilization of an appropriate viscosity model, and inclusion of the wall elasticity [9].

2. Literature Review

In many previous studies, computational fluid dynamics (CFD) simulation in three dimensional models derived from anatomic medical images has been employed to investigate the blood flow in the carotid artery [9]. Due to the complex nature of the diseased carotid bifurcation and its effect on the blood flow patterns, studies utilizing patient-specific geometries are important [16]. Recently, Saxena *et. al*. [21] used Active Dynamic Thermography (ADT) method to detect the presence of stenosis in the carotid artery. Remarkably, Lopes *et. al*. [19] presented an extensive systematic literature review of carotid artery numerical simulation with patient-specific geometries.

Based on our literature survey, the carotid artery CFD numerical simulations can be classified into three major categories. Firstly, the consideration of flow model is either laminar or defined by a turbulence model. Secondly, the viscosity model consideration is either Newtonian, Non-Newtonian or both for comparison. Thirdly, the geometry of carotid artery is either non-stenotic, stenotic or both for comparison. These three classification of previous studies conducted in the span of 6 years from year 2004 to 2020 are summarized in Table 1.

The consideration of blood as a non-Newtonian fluid is recommended by several studies due to significant different results of hemodynamic parameters between the Newtonian and non-Newtonian. According to Bouteloup *et. al*. [3], the non-Newtonian models should follow appropriate limits otherwise the non-Newtonian effects may be overestimated.

From the summary in Table 1, most of the previous studies considered laminar flow model and only one study used the K-ε turbulence model. This is due the assumption that blood flow is laminar based on calculated Renolds number is lower than 2000. However, there is high possibilities that flow may change to a transitional or even turbulent in the case of severely stenosed geometries [19]. Besides that, the previous CFD studies that compared hemodynamics of non-stenosed with stenosed artery assumed that the flow is laminar. Therefore, CFD numerical simulation that compare non-stenosed and stenosed carotid artery with appropriate turbulence model remains as a research gap in this field of study.

Thus, this study is intended to investigate the effect of various degree and position (pre-bifurcation and post-bifurcation) of stenosis on carotid artery hemodynamics through realistic CFD numerical simulations with appropriate turbulence model.

Table 1
Carotid Artery CFD Numerical Simulations

Authors	Flow Model	Viscosity Model	Stenosis
Bouteloup et. al. [3]	K-ε	Newtonian	Stenotic
Nagargoje et. al. [20]	Laminar	Newtonian	Non-stenotic
Lopes et. al. [18]	Laminar	Newtonian	Non-stenotic
Sia et. al. [22]	Laminar	Newtonian	Stenotic
Lee et. al. [15]	Laminar	Both	Non-stenotic
Azar et. al. [2]	Laminar	Non-Newtonian	Stenotic
Yao et. al. [26]	Laminar	Newtonian	Non-stenotic
Kumar et. al. [14]	Laminar	Both	Stenotic
Li et. al. [16]	Laminar	Newtonian	Both
Guerciotti and Vergara et. al. [11]	Laminar	Both	Stenotic
Domanin et. al. [6]	Laminar	Newtonian	Non-stenotic
Urevc et. al. [25]	Laminar	Both	Non-stenotic
Bit et. al. [4]	Laminar	Both	Both
Conti et. al. [5]	Laminar	Newtonian	Both
Gallo et. al. [8]	Laminar	Newtonian	Non-stenotic
Sousa et. al. [23]	Laminar	Newtonian	Both
Gharahi et. al. [9]	Laminar	Both	Both
Guerciotti et. al. [10]	Laminar	Newtonian	Both
Harrison et. al. [12]	Laminar	Newtonian	Non-stenotic
Fu et. al. [7]	Laminar	Newtonian	Stenotic

3. Methodology

The blood rheological properties were assumed as incompressible and Newtonian fluid, which is valid under large scale flow [3]. The CFD numerical simulations were conducted based on a general-purpose, finite volume, Navier-Stokes solver, ANSYS Fluent (17.0) software. A 3 dimensional model of a non-stenotic carotid artery model from previous study as shown in Figure 1(a), which was created through patient specific Computed Tomography (CT) scanning of luminal casting was used this investigation.

The surfaces of the boundaries are shown in the same figure, where the inlet is blood entering through the distal boundary of Common Carotid Artery (CCA), outlets are at the ICA and ECA. For transient simulations, the inlet and outlet boundary conditions are formulated by extracting few significant sample data from boundary condition used by Lopes *et. al*. [18] as shown in Figure 1(b). Figure 1(c) shows the extracted volume flowrate for 1 cardiac cycle used to formulate the velocity inlet boundary condition simply by dividing the volume flowrate by Inlet area ($3.0868e^{-5}\ m^2$) of the artery model, where the peak systole velocity is 0.583 m/s at, t = 0.2s. Figure 1(d) shows the boundary condition of pressure outlets at both ICA and ECA for 1 cardiac cycle, where the maximum pressure occurs at, t = 0.45s.

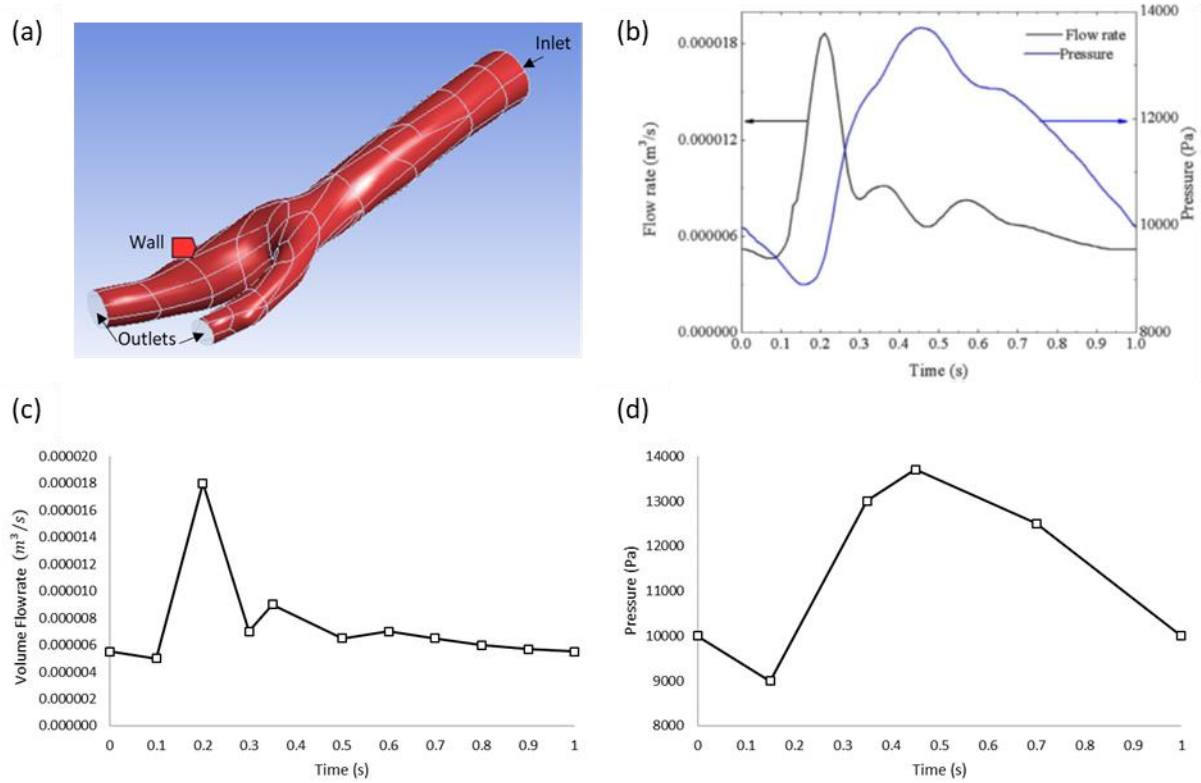

Fig. 1. Boundary Conditions, (a) Boundaries, (b) Lopes *et. al*. [18], (c) Inlet and (d) Outlet

For the steady state simulations, a constant inlet velocity of 0.583 m/s, and with an outflow and a reference pressure of 9332.54 Pa was imposed. The flow rate weighting for ICA and ECA outlets were set to be 0.6959 and 0.3044, respectively based the results of mass flow separation from CFD simulation conducted by Lopes *et. al*. [18]. For both transient and steady simulation, the wall boundary condition was assumed to be rigid with no-slip condition, the density and viscosity of blood are 1060 kg/m^3 [18] and 0.004 Pa.s [3], respectively. The meshing was done in ANSYS Meshing with 10 number of boundary layers with maximum thickness of 0.5 mm was imposed near to the wall as shown in Figure 2 (a) and 2 (b). Figure 2 (c) shows a mesh convergence of 0.06% is achieved through grid independent test conducted with several sets of mesh by evaluating ICA maximum velocity for each mesh. The final mesh has a total of 703812 elements.

Considering maximum velocity of 0.583 m/s, the Reynolds number calculated from Equation 1 [18] is 968, which may be reasonable to assume that the flow is laminar.

$$Re = \rho VD/\mu \quad (1)$$

However, in this study, several turbulence models have been tested. Along with Laminar flow model, steady state simulations were conducted with two equations Standard k-ε, Standard k-ω, SST k-ω with Low-Reynolds number correction and seven equation Reynolds Stress Model (RSM) for the non-stenotic artery model.

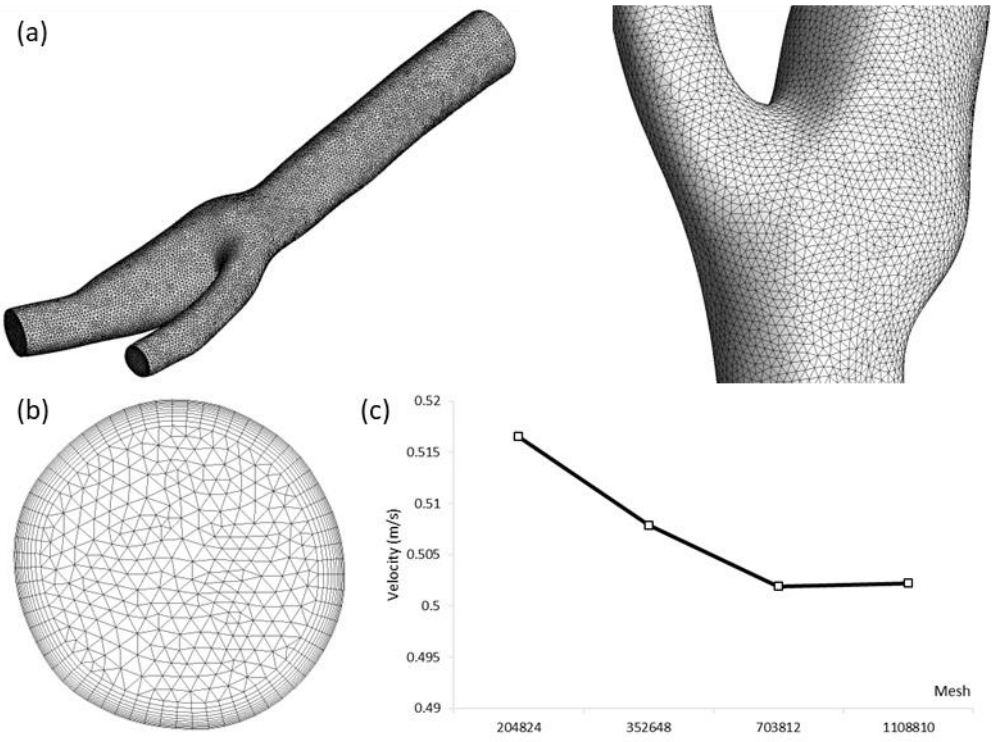

Fig. 2. (a) Meshed Model, (b) Boundary Layer (Inlet) and (c) Grid Independent Test

In order to evaluate the effect of various degree (30% and 70%) and position of stenosis in carotid artery, the non-stenotic artery geometry was altered in ANSYS *Designmodeller*. The pre-bifurcation stenosis was modelled with an assumption that the stenosis shape is approximately semi-circle with gradually decreasing followed by increasing cross-section area in the direction from inlet to the bifurcation in all 3-dimensions. Figure 3 (a) shows the cross section of CCA at the plane where the pre-bifurcation stenosis is modelled. The term 30% and 70% for pre-bifurcation stenosis is defined by the ratio of stenosis radius blocking the blood flow to the cross section radius of the healthy model as shown in Figure 3 (a). Figure 3 (b) and (c) shows the side view and cross section of stenosis center for 30% and 70% pre-bifurcation stenosis, respectively.

The post-bifurcation stenosis was modelled with an assumption that the stenosis is spherical because the semi-circle shaped stenosis is not appropriate for stenosis at ICA because the carotid sinus (bulb) has more tendency of plaque formation unlike pre-bifurcation stenosis which usually form around the circumference of CCA. Figure 3 (d) shows an instance, if there is a stenosis of 100% blocking the flow in ICA, the diameter of the spherical shape stenosis would be 6.93mm. Therefore, a spherical shaped stenosis with diameter of 4.851mm and 2.079mm was created, hence blocking the flow by 70% and 30% as shown in Figure 3 (e) and (f), respectively. Several studies such as Lopes et. al. and Li et. al. (2019) has shown that the carotid sinus has high tendency for stenosis formation due to low Wall Shear Stress (WSS). Thus, the post-bifurcation stenosis is modelled only at the bulb (carotid sinus) and the consideration of stenosis at ECA is neglected.

Figure 4(a) shows the non-stenotic artery. Figure 4(b) and 4(c) are the arteries with 30% and 70% pre-bifurcation stenosis, respectively. Figure 4(d) and 4(e) are the arteries with 30% and 70% post-bifurcation stenosis, respectively. These models of the arteries, Non-stenotic, PreST-30%, PreST-70%, PostST-30%, PostST-70% are denoted as M1, M2, M3, M4 and M5, respectively as nomenclature.

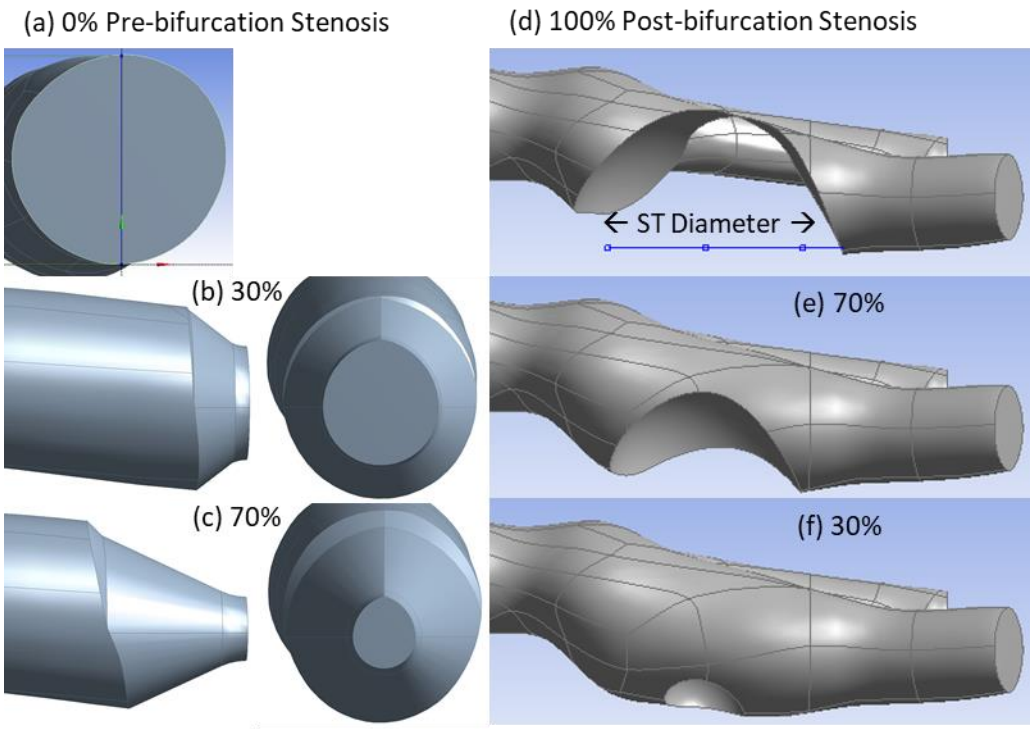

Fig. 3. (a) CCA Cross-section, (b) PreST-30%, (c) PreST-70%, (d) PostST-100%, (e) PostST-70% and (f) PostST-30%

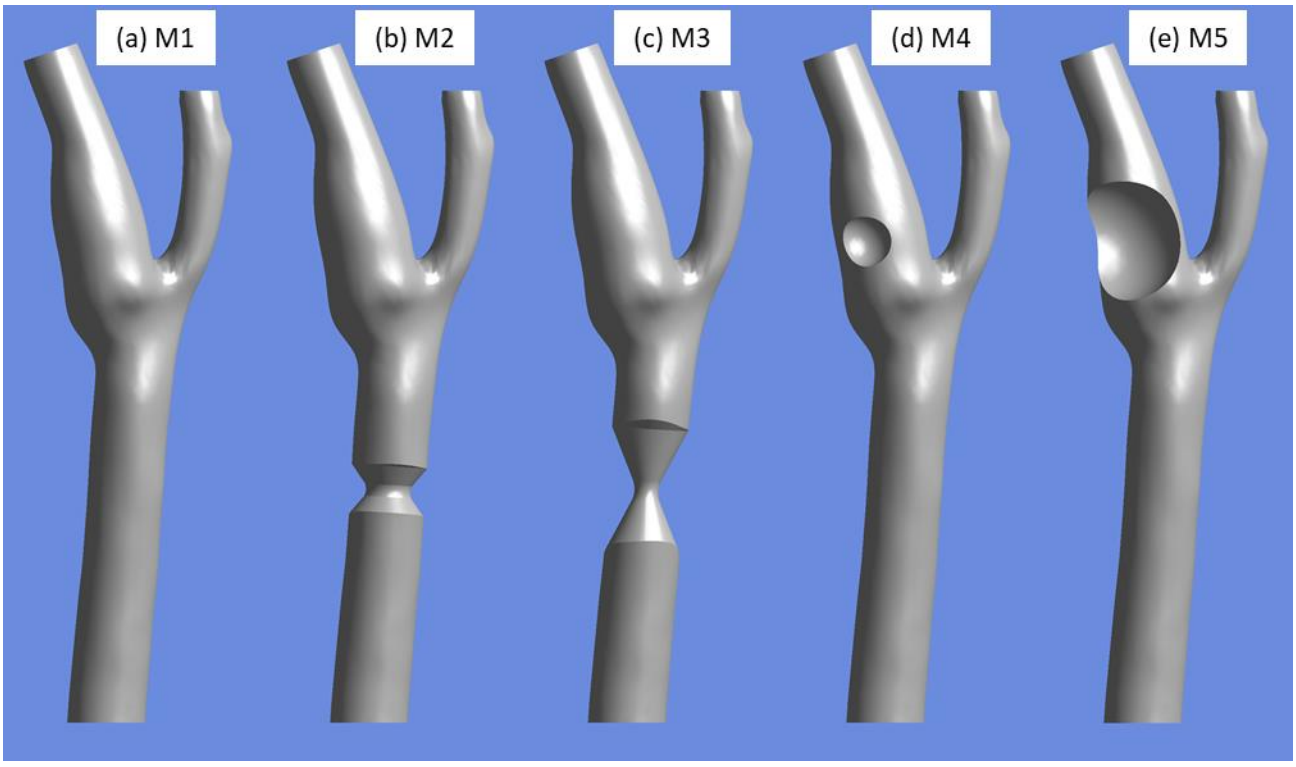

Fig. 4. (a) Non-stenotic (b) PreST-30% (c) PreST-70% (d) PostST-30% (e) PostST-70%

Transient simulations were conducted for each artery models (M1 to M5). The SST k-ω turbulence model with Low-Reynolds number correction was used for the reason that this model found to be more appropriate compared to other flow models. The transient simulations were performed for 3 cardiac cycles with step size of 0.01s for a total flow time of 3s. The results of the third cardiac cycle were exported, analyzed and presented here.

4. Results

Figure 5 (a) to (e) shows the results of velocity streamline for Laminar, Standard k-ε, Standard k-ω, SST k-ω with Low-Reynolds number and Reynolds Stress model, respectively.

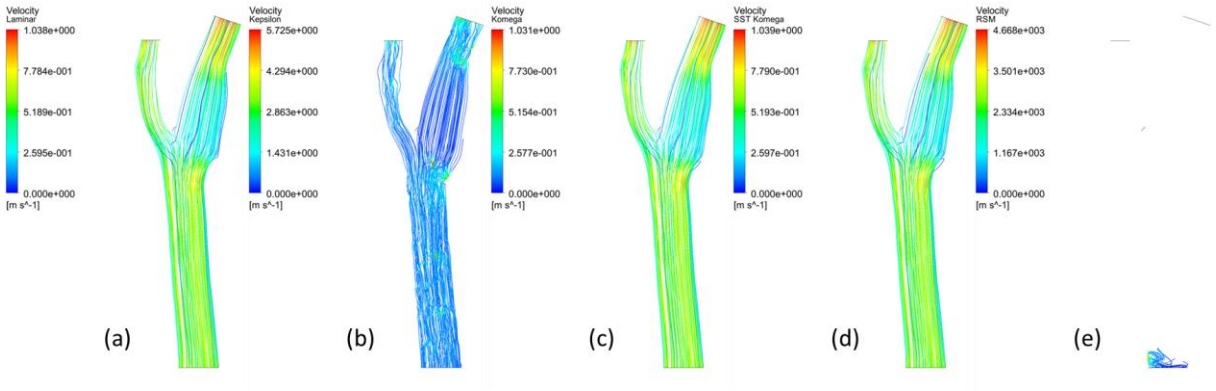

Fig. 5. Velocity Streamline of non-Stenotic Artery by different Turbulence Models, (a) Laminar (b) K-ε (c) K-ω (d) SST K-ω and (e) RSM

As the blood flow condition is laminar based on the calculated Reynolds number and the usage of turbulence model is only to predict the turbulent flow stream. From the result, the Reynolds Stress model failed to compute the velocity streamline as shown in Figure 4 (e) and the Standard k-ε model over predicts the flow velocity as shown in Figure 4 (d). This shows the limitation of k-ε turbulence model at determining near the wall-quantities, flows with Low-Reynolds values and that exhibit strong curvatures as reported by several studies [13,17,27].

The standard k-ω and SST k-ω predicted velocity magnitude at a reasonable range, where flow streamline was predicted with the magnitude remain similar to Laminar model as shown in Figure 5 (c) and 5 (d), respectively. This shows the accuracy of K-ω model in predicting flow quantities at Low-Reynolds numbers. Although the Standard and SST k-ω are both reasonable, however the velocity predicted by SST k-ω with low-Re is closer to laminar than the Standard k-ω model. Therefore, the SST k-ω with Low-Reynolds number correction was used for the transient simulations to investigate the effect of stenosis condition.

Figure 6 (a) and (b) shows the results of Maximum Velocity at ICA and ECA, respectively for 1 cardiac cycle for M1, M2, M3, M4 and M5.

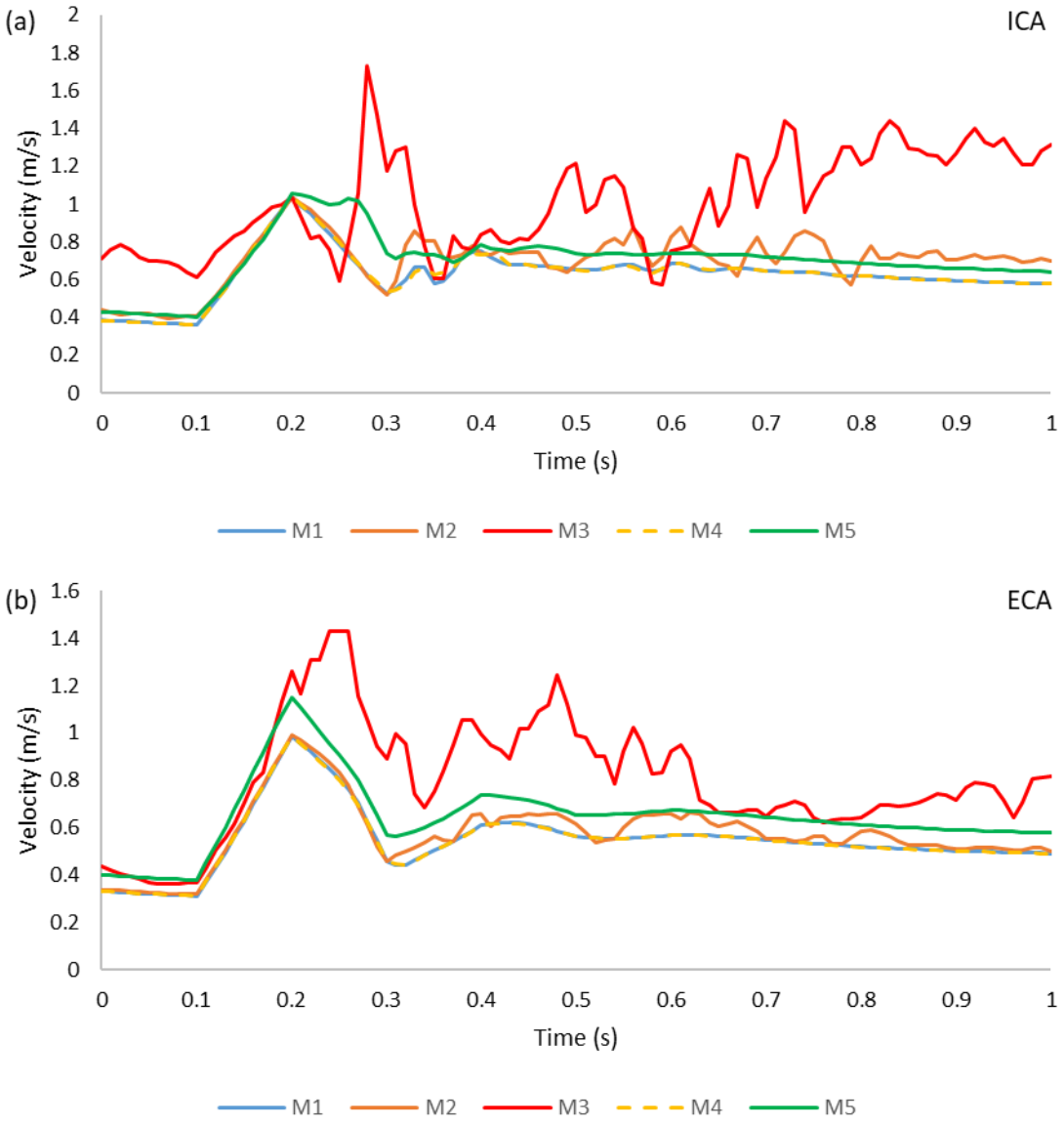

Fig. 6. Maximum Velocity at (a) ICA and (b) ECA

Considering time averaged difference of maximum velocity in comparison to healthy case, as the degree of pre-bifurcation stenosis increases from 30% to 70%, the ICA maximum velocity increased from 12% to 65%. Also, the ECA maximum velocity increased from 5% to 45%, respectively. As the degree of post-bifurcation stenosis increases to 30%, the ECA maximum velocity decreased by 0.16%, however in the 70% stenosis case, the ECA maximum velocity increased by 19%. In addition, in the 70% post-bifurcation stenosis case, the ICA maximum velocity does not reduce immediately after the peak systole velocity (at time = 0.2s), instead it fluctuates and then decrease rapidly. This can be seen in Figure 7 which shows the ICA velocity contour for 1 cardiac cycle for M1 and M5 indicating maximum velocity at each time.

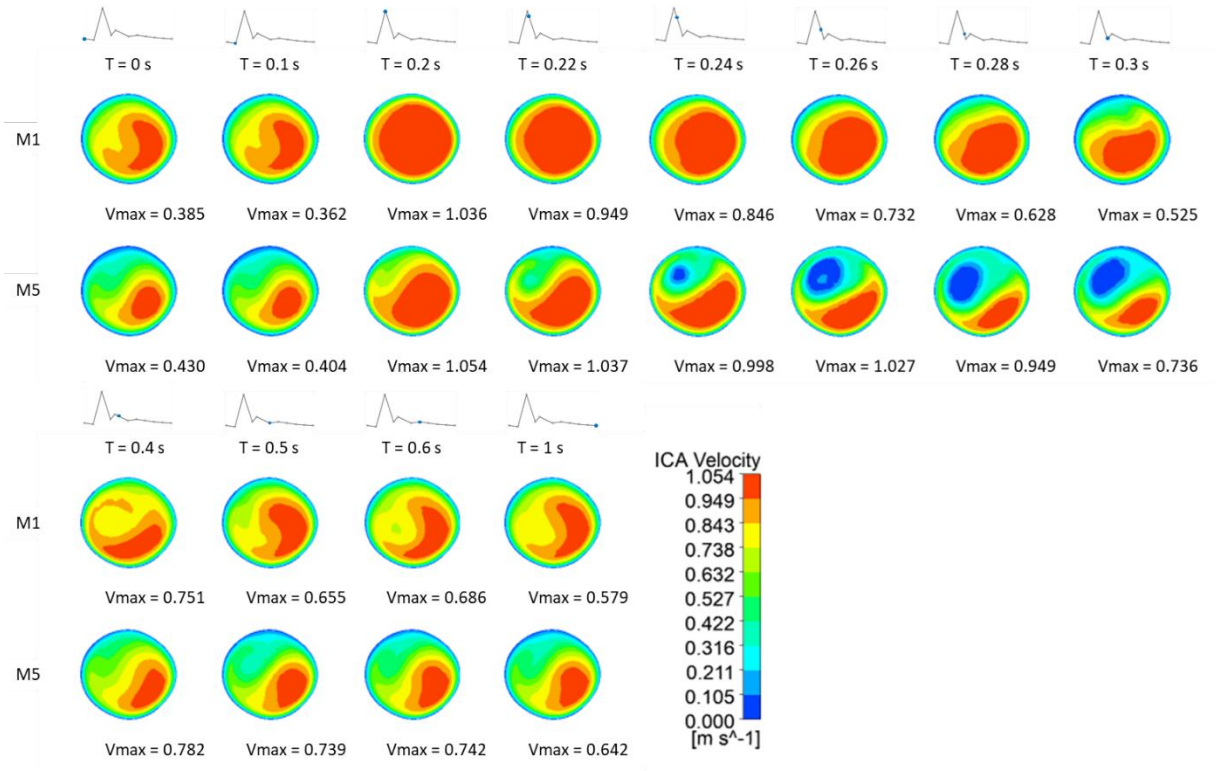

Fig. 7. ICA Velocity for M1 and M5 indicating maximum velocity (m/s) at each time

After the peak systole velocity at 0.2s, the ICA maximum velocity of M5 reduces to 0.998 m/s at 0.24s but increased again to 1.027 m/s at 0.26s. Also, the loss of flow velocity at the blocked section can be seen throughout the cardiac cycle, especially from 0.24s to 0.3s.

The ratio of ICA and ECA velocity to inlet velocity at the peak velocity (0.2s) was computed here, as calculated by Bouteloup *et. al*. [3]. Figure 8 (a), (b), (c) and (d) shows the results of Velocity Ratio at 0.2s (peak) measured along ICA Horizontal Line, ECA Horizontal Line, ICA Vertical Line and ECA Vertical Line, respectively, for M1, M2, M3, M4 and M5. Where, the non-dimensional distance (r/Ro) is the ratio of distance where measurement was taken from the center of ICA and ECA to the radius of ICA and ECA, respectively.

Considering maximum difference of velocity ratio in comparison to healthy case, as the degree of pre-bifurcation stenosis increases to 70%, the ICA velocity ratio decreases by 22% and 21% along the ICA horizontal and vertical line, respectively. Yet, the ECA velocity ratio increases by 101% at non-dimensional distance (r/Ro) = -0.98 along the ECA horizontal line and 65% along the vertical line. As the degree of post-bifurcation stenosis increases to 70%, the ICA velocity ratio along the horizontal line decreases by 16% at the outer wall of ICA. Also, along the vertical line, it decreases by 34% at the upper wall of ICA. As the degree of post-bifurcation stenosis increases, the ECA velocity ratio increases by 28%.

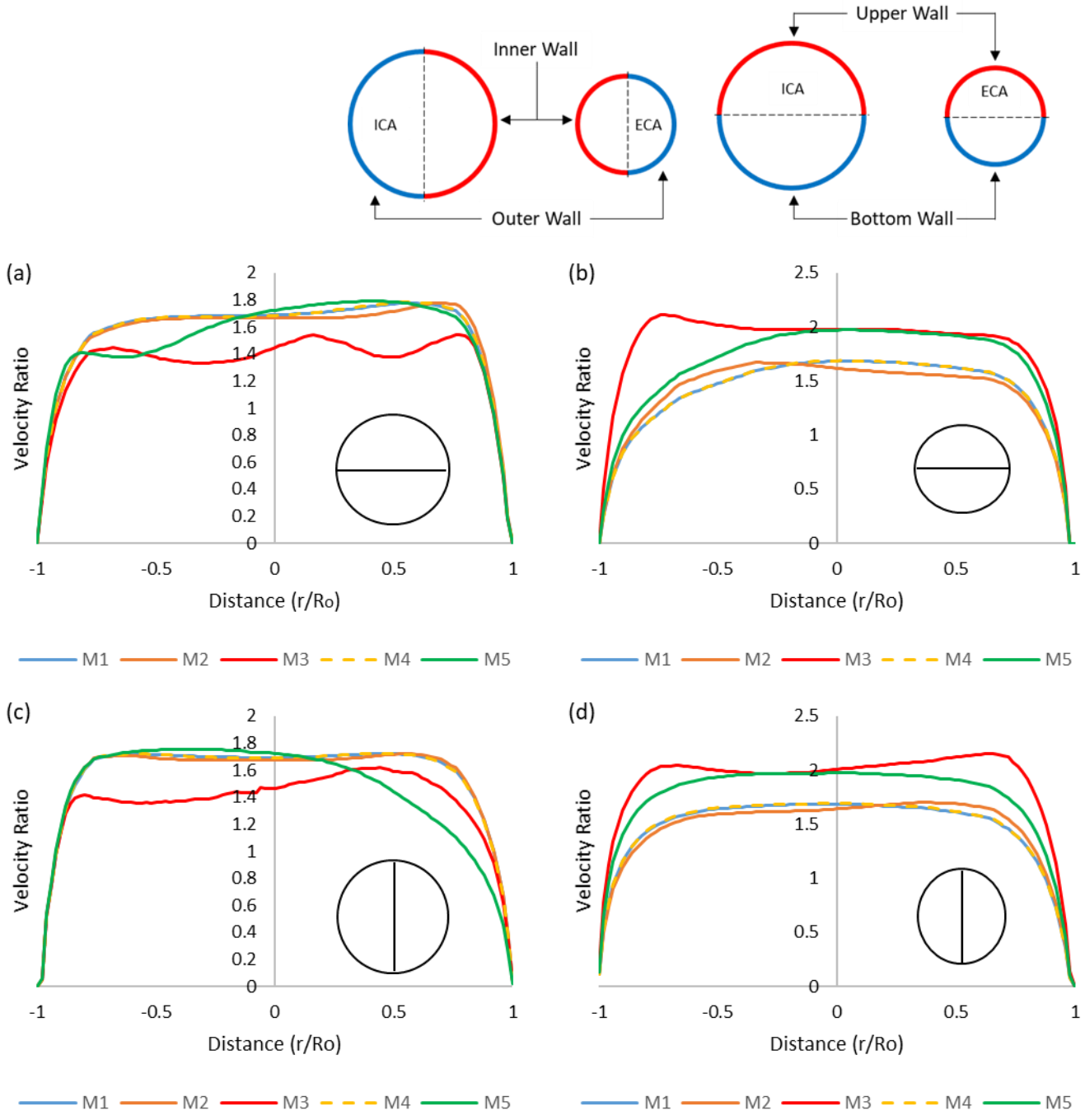

Fig. 8. Velocity Ratio at 0.2s measured at (a) ICA Horizontal, (b) ECA Horizontal, (c) ICA Vertical and (d) ECA Vertical

5. Conclusion

As the study intended to investigate the effect of various degree and position of stenosis on carotid artery hemodynamics, from the results obtained from the CFD numerical simulations, several conclusions can be derived as follow:

1. As the degree of pre-bifurcation stenosis increases from 30% to 70%, the ICA maximum velocity increases from 12% to 65%. Also, the ECA maximum velocity increases from 5% to 45%.

2. As the degree of post-bifurcation stenosis increases to 30%, the ECA maximum velocity decreased slightly by 0.16%, however in the 70% stenosis case, the ECA maximum velocity increased by 19%.

3. As the degree of pre-bifurcation stenosis increases to 70%, the ICA velocity ratio decreases by 22% and 21% along the ICA horizontal and vertical line, respectively. Yet, the ECA velocity ratio increases by 101% along the ECA horizontal line and 65% along the vertical line.

4. As the degree of post-bifurcation stenosis increases to 70%, the ICA velocity ratio along the horizontal line decreases by 16% at the outer wall of ICA. Also, along the vertical line, it decreases by 34% at the upper wall of ICA. However, the ECA velocity ratio increased by 28%.

Acknowledgement
This work was supported by the Ministry of Higher Education Malaysia, under project grant FRGS/1/2018/TK03/UKM/02/5. All types of support from Universiti Kebangsaan Malaysia are also gratefully acknowledged.

References

[1] Abugattas, C., A. Aguirre, E. Castillo, and M. Cruchaga. "Numerical study of bifurcation blood flows using three different non-Newtonian constitutive models." *Applied Mathematical Modelling* 88 (2020): 529-549.

[2] Azar, Dara, William M. Torres, Lindsey A. Davis, Taylor Shaw, John F. Eberth, Vijaya B. Kolachalama, Susan M. Lessner, and Tarek Shazly. "Geometric determinants of local hemodynamics in severe carotid artery stenosis." *Computers in biology and medicine* 114 (2019): 103436.

[3] Bouteloup, Hugo, Johann Guimaraes de Oliveira Marinho, and Daniel M. Espino. "Computational analysis to predict the effect of pre-bifurcation stenosis on the hemodynamics of the internal and external carotid arteries." *Journal of Mechanical Engineering and Sciences* 14, no. 3 (2020): 7029-7039.

[4] Bit, Arindam, Dushali Ghagare, Albert A. Rizvanov, and Himadri Chattopadhyay. "Assessment of influences of stenoses in right carotid artery on left carotid artery using wall stress marker." *BioMed Research International* 2017 (2017).

[5] Conti, Michele, Chris Long, Michele Marconi, Raffaella Berchiolli, Yuri Bazilevs, and Alessandro Reali. "Carotid artery hemodynamics before and after stenting: A patient specific CFD study." *Computers & Fluids* 141 (2016): 62-74.

[6] Domanin, Maurizio, Daniele Bissacco, Davide Le Van, and Christian Vergara. "Computational fluid dynamic comparison between patch-based and primary closure techniques after carotid endarterectomy." *Journal of Vascular Surgery* 67, no. 3 (2018): 887-897.

[7] Fu, Yulin, Aike Qiao, and Long Jin. "The influence of hemodynamics on the ulceration plaques of carotid artery stenosis." *Journal of Mechanics in Medicine and Biology* 15, no. 01 (2015): 1550008.

[8] Gallo, Diego, David A. Steinman, and Umberto Morbiducci. "Insights into the co-localization of magnitude-based versus direction-based indicators of disturbed shear at the carotid bifurcation." *Journal of biomechanics* 49, no. 12 (2016): 2413-2419.

[9] Gharahi, Hamidreza, Byron A. Zambrano, David C. Zhu, J. Kevin DeMarco, and Seungik Baek. "Computational fluid dynamic simulation of human carotid artery bifurcation based on anatomy and volumetric blood flow rate measured with magnetic resonance imaging." *International journal of advances in engineering sciences and applied mathematics* 8, no. 1 (2016): 46-60.

[10] Guerciotti, Bruno, Christian Vergara, Laura Azzimonti, Laura Forzenigo, Adelaide Buora, Piero Biondetti, and Maurizio Domanin. "Computational study of the fluid-dynamics in carotids before and after endarterectomy." *Journal of biomechanics* 49, no. 1 (2016): 26-38.

[11] Guerciotti, Bruno, and Christian Vergara. "Computational comparison between Newtonian and non-Newtonian blood rheologies in stenotic vessels." In *Biomedical Technology*, pp. 169-183. Springer, Cham, 2018.

[12] Harrison, Gareth J., Thien V. How, Robert J. Poole, John A. Brennan, Jagjeeth B. Naik, S. Rao Vallabhaneni, and Robert K. Fisher. "Closure technique after carotid endarterectomy influences local hemodynamics." *Journal of Vascular Surgery* 60, no. 2 (2014): 418-427.

[13] Khalili, Fardin, Peshala Gamage, and Hansen A. Mansy. "Verification of turbulence models for flow in a constricted pipe at low reynolds number." *arXiv preprint arXiv:1803.04313* (2018).

[14] Kumar, Nitesh, Abdul Khader, Raghuvir Pai, Panayiotis Kyriacou, Sanowar Khan, and Prakashini Koteshwara. "Computational fluid dynamic study on effect of Carreau-Yasuda and Newtonian blood viscosity models on hemodynamic parameters." *Journal of Computational Methods in Sciences and Engineering* 19, no. 2 (2019): 465-477.

[15] Lee, Sang Hyuk, Kap-Soo Han, Nahmkeon Hur, YOUNG I. CHO, and Seul-Ki Jeong. "THE EFFECT OF PATIENT-SPECIFIC NON-NEWTONIAN BLOOD VISCOSITY ON ARTERIAL HEMODYNAMICS PREDICTIONS." *Journal of Mechanics in Medicine and Biology* 19, no. 08 (2019): 1940054.

[16] Li, Cong-Hui, Bu-Lang Gao, Ji-Wei Wang, Jian-Feng Liu, Hui Li, and Song-Tao Yang. "Hemodynamic factors affecting carotid sinus atherosclerotic stenosis." *World Neurosurgery* 121 (2019): e262-e276.

[17] Liu, X., X. Zhou, X. Hao, and X. Sang. "Modified numerical simulation model of blood flow in bend." *The West Indian Medical Journal* 64, no. 5 (2015): 495.

[18] Lopes, D., Hélder Puga, J. Carlos Teixeira, and S. F. Teixeira. "Influence of arterial mechanical properties on carotid blood flow: Comparison of CFD and FSI studies." *International Journal of Mechanical Sciences* 160 (2019): 209-218.

[19] Lopes, D., Hélder Puga, J. Teixeira, and R. Lima. "Blood flow simulations in patient-specific geometries of the carotid artery: A systematic review." *Journal of Biomechanics* 111 (2020): 110019.

[20] Nagargoje, Mahesh, and Raghvendra Gupta. "Effect of sinus size and position on hemodynamics during pulsatile flow in a carotid artery bifurcation." *Computer Methods and Programs in Biomedicine* 192 (2020): 105440.

[21] Saxena, Ashish, E. Y. K. Ng, and Soo Teik Lim. "Active dynamic thermography to detect the presence of stenosis in the carotid artery." *Computers in Biology and Medicine* 120 (2020): 103718.

[22] Sia, Sheau Fung, Xuemei Zhao, Yong Yu, and Yu Zhang. "Multiphase particle-in-cell simulation in severe internal carotid artery stenosis." *Powder Technology* 358 (2019): 62-67.

[23] Sousa, Luísa C., Catarina F. Castro, Carlos C. António, Fernando Sousa, Rosa Santos, Pedro Castro, and Elsa Azevedo. "Computational simulation of carotid stenosis and flow dynamics based on patient ultrasound data–A new tool for risk assessment and surgical planning." *Advances in medical sciences* 61, no. 1 (2016): 32-39.

[24] Tu, Jiyuan, Kelvin KL Wong, Sherman CP Cheung, Richard Beare, and Thanh Phan. "Analysis of patient-specific carotid bifurcation models using computational fluid dynamics." *Journal of Medical Imaging and Health Informatics* 1, no. 2 (2011): 116-125.

[25] Urevc, Janez, Iztok Žun, Milan Brumen, and Boris Štok. "Modeling the effect of red blood cells deformability on blood flow conditions in human carotid artery bifurcation." *Journal of Biomechanical Engineering* 139, no. 1 (2017): 011011.

[26] Yao, Xinke, Zhengze Dai, Xu Zhang, Jie Gao, Gelin Xu, Yan Cai, and Zhiyong Li. "Carotid Geometry as a Predictor of In-Stent Neointimal Hyperplasia—A Computational Fluid Dynamics Study—." *Circulation Journal* (2019): CJ-18.

[27] Zhou, Lixing. *Theory and modeling of dispersed multiphase turbulent reacting flows*. Butterworth-Heinemann, 2018.